

<https://doi.org/10.1038/s43247-024-01446-z>

Metal mobilization from thawing permafrost to aquatic ecosystems is driving rusting of Arctic streams

Check for updates

Jonathan A. O'Donnell¹✉, Michael P. Carey², Joshua C. Koch², Carson Baughman², Kenneth Hill³, Christian E. Zimmerman², Patrick F. Sullivan⁴, Roman Dial⁵, Timothy Lyons⁶, David J. Cooper⁷ & Brett A. Poulin⁸

Climate change in the Arctic is altering watershed hydrologic processes and biogeochemistry. Here, we present an emergent threat to Arctic watersheds based on observations from 75 streams in Alaska's Brooks Range that recently turned orange, reflecting increased loading of iron and toxic metals. Using remote sensing, we constrain the timing of stream discoloration to the last 10 years, a period of rapid warming and snowfall, suggesting impairment is likely due to permafrost thaw. Thawing permafrost can foster chemical weathering of minerals, microbial reduction of soil iron, and groundwater transport of metals to streams. Compared to clear reference streams, orange streams have lower pH, higher turbidity, and higher sulfate, iron, and trace metal concentrations, supporting sulfide mineral weathering as a primary mobilization process. Stream discoloration was associated with dramatic declines in macroinvertebrate diversity and fish abundance. These findings have considerable implications for drinking water supplies and subsistence fisheries in rural Alaska.

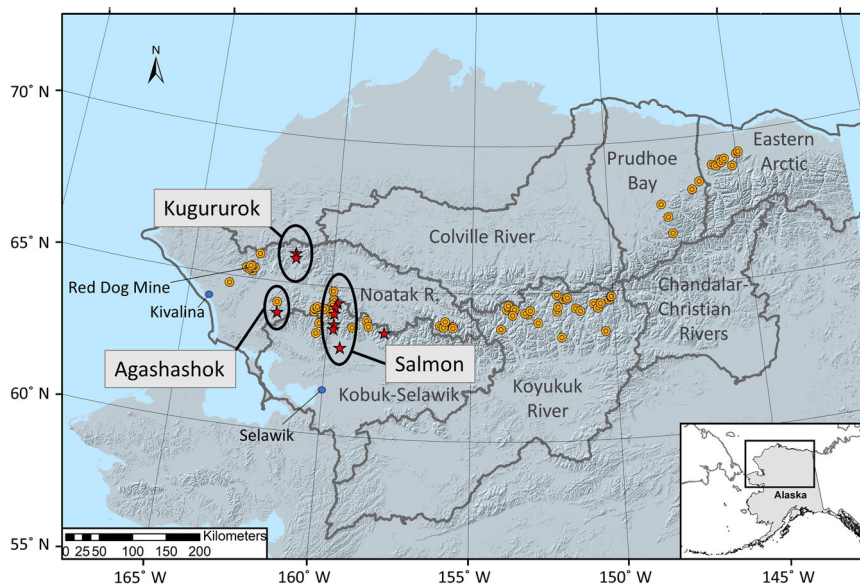
Rapid warming of the Arctic is altering hydrological, biogeochemical, and ecological linkages between terrestrial and aquatic ecosystems¹. Arctic soils contain large amounts of organic carbon, nutrients, mercury and other metals, much of which are stored in perennially frozen ground, or permafrost^{2–4}. Warming and increased snowfall is causing widespread permafrost thaw⁵, which alters and generates new hydrologic flow paths, can alter soil and bedrock weathering patterns, and mobilizes thawed chemical constituents for transport from soils to streams and rivers^{6–8}. An emergent phenomenon threatens pristine streams across Alaska's Brooks Range, with implications across the circum-Arctic^{9–11}, specifically surface waters that are abruptly changing from clear to orange color, indicating a shift to an impaired state (Fig. 1). While considerable research has focused on the fate of carbon and nutrients transported from permafrost to aquatic ecosystems¹², few studies have focused on the causes of iron (Fe) and trace metal mobilization from thawing soils to streams^{13,14} and less is known about the consequences for water quality and aquatic food webs. Abrupt transitions in water chemistry on the timescale of weeks to months may represent an unforeseen risk of permafrost thaw for food security¹⁵, as subsistence

fisheries and drinking water supplies may become degraded in some Arctic river networks.

Recent observations from the Arctic indicate that waters draining permafrost landscapes may be vulnerable to the mobilization of Fe and other metals following thaw through changing redox conditions and microbial activity^{13,14,16} and enhanced chemical weathering of minerals^{9,17}. One striking indication of altered Fe-cycling processes is the abrupt change in the color of streams that reflects a dramatic shift in water quality¹⁸. For example, the release of reduced Fe (Fe(II)) from thawing permafrost and its subsequent oxidation to Fe(III) particulates in surface waters has been documented in a small watershed on the North Slope of Alaska¹³. Elevated Fe(III) particulates and the products of mineral weathering reactions (e.g., sulfuric acid, toxic trace metals) degrade water quality by increasing turbidity, decreasing pH, and increasing concentrations of metals acutely toxic to stream biota¹⁹. Additional observations of stream discoloration were recently published in an opinion piece on the Salmon River¹⁸, a National Wild and Scenic River in northwest Alaska, following reports of its waters abruptly shifting from clear to orange in a manner resembling acid-mine drainage.

¹National Park Service, Arctic Network, 240 W 5th Avenue, Anchorage, AK 99504, USA. ²U.S. Geological Survey, Alaska Science Center, 4210 University Drive, Anchorage, AK 99508, USA. ³National Park Service, Arctic and Central Alaska Networks, 4175 Geist Rd., Fairbanks, AK 99775, USA. ⁴University of Alaska Anchorage, Environment and Natural Resources Institute, 3151 Alumni Drive, Anchorage, AK 99508, USA. ⁵Alaska Pacific University, Institute of Culture and Environment, 4101 University Drive, Anchorage, AK 99508, USA. ⁶University of California-Riverside, Department of Earth & Planetary Sciences, 900 University Ave., Riverside, CA 92521, USA. ⁷Colorado State University, Department of Forest and Rangeland Stewardship, Fort Collins, CO 80523, USA. ⁸University of California Davis, Department of Environmental Toxicology, 1 Shields Avenue, Davis, CA 95616, USA. ✉e-mail: jaodonnell@nps.gov

Fig. 1 | Map of orange stream observations across the Brooks Range in northern Alaska. Orange circles indicate orange stream observations, red stars indicate sites where water samples were collected (Fig. 2)²⁰, and blue circles are nearby villages. Hydrologic Unit Code-6 (HUC) basins are shown as black outlines from the National Watershed Boundary dataset⁶⁷. The hill-shade layer utilizes the USGS National Elevation Dataset⁶⁸. Map generated in Esri ArcMap software. Map credit: Kenneth Hill, NPS.



In this study, we document 75 streams across northern Alaska that recently shifted from clear to orange (Supplementary Table 1). The primary objectives are to describe changes and explore the potential causes of recent stream impairment in Alaska's Brooks Range, identify the timing of shifts in water quality (pH, Fe, trace metals, sulfate), and assess the consequences for aquatic ecosystems. Remote sensing observations of a subset of impaired streams constrain the timing of rapid and widespread stream discoloration to the last 5–10 years. Further, field and laboratory measurement document drastic shifts in the chemical composition of impaired rivers and the degradation of stream habitat. Using these observations, we discuss the state of the science and introduce the broad interdisciplinary components of this phenomenon, including (1) the spatial extent and recent onset of stream discoloration; (2) possible causes, including the critical role of recent climate change-induced permafrost thaw; (3) underlying geochemical processes and potential impacts on stream water quality; and (4) consequences for stream biota. Most importantly, this study could inform additional research directions and strategies.

Results and discussion

Observations of orange streams in Alaska's Brooks Range

To characterize the spatial extent of orange streams in Alaska's Brooks Range, we reviewed remotely sensed imagery to validate crowd-sourced observations from federal and state scientists, academic researchers, local pilots, wilderness guides and recreationists, and rural and Indigenous communities (Supplementary Table 1). Orange streams have been observed across much of northern Alaska, spanning traditional territories of the Alaska Native peoples in the Noatak, Kobuk, and Koyukuk River basins; public lands; designated wilderness; and within watersheds of several National Wild and Scenic Rivers, including the Alatna, John, Koyukuk, Tinayguk, and Salmon rivers. To date, we have documented 75 altered headwater tributaries in 41 higher order river catchments with visible impairment (Supplementary Table 1). Their distribution spans nearly 1,000 km, from the lower Noatak River basin in the west to the Arctic National Wildlife Refuge in the northeast (Fig. 1). Nearly all orange streams occur in remote areas, tens to hundreds of kilometers from land-use impacts such as mining or roads.

Geochemical consequences of trace metal mobilization

Little is currently known about the chemical composition of recently degraded streams in the Brooks Range, as previous studies have focused on gradual, multi-decadal shifts in the chemistry of Arctic rivers⁷. However, the presence of orange precipitates along river corridors points to mobilization

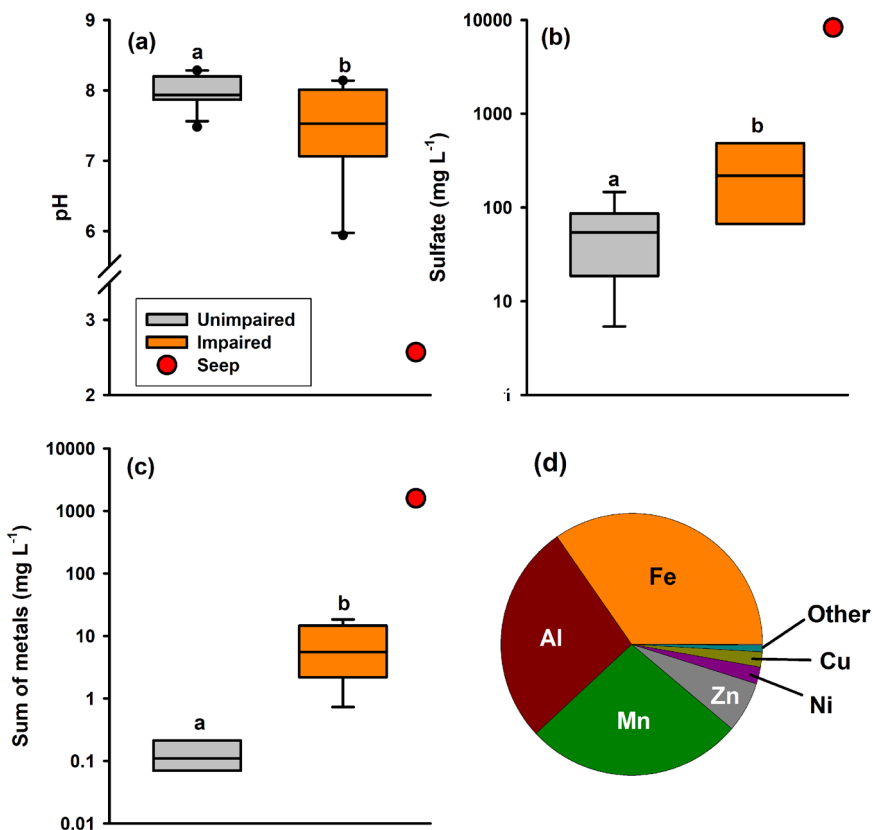
of at least Fe from catchment soils. To assess the chemical composition of orange streams, water samples from the Agashashok, Kugururok, and Salmon rivers were collected during the summer of 2022 from discolored reaches ($n = 10$) and compared to samples collected from nearby reference streams ($n = 13$; Supplementary Fig. 1)²⁰. These three rivers were selected for water sampling because (1) they were within watersheds with existing monitoring locations as part of the National Park Service's Arctic Inventory & Monitoring program, (2) we had directly observed orange streams within each watershed, and (3) they were accessible via helicopter or fixed-wing aircraft from Kotzebue, Alaska.

In our study, orange streams had lower pH (mean pH \pm standard deviation = 7.41 ± 0.75) compared to reference streams (7.98 ± 0.24 ; two-tailed t test: $t = 2.510$, $df = 20$, $P = 0.035$; Fig. 2a) and other comparable unimpaired stream and rivers across the region²¹. Lower pH values in the orange streams are likely due to the input of Fe-containing water of substantially lower pH into the stream system. The pH would be higher in the affected orange stream compared to the acidic input because of mixing and/or buffering effects. For example, we sampled a recently formed terrestrial seep in the Agashashok River basin that was highly acidic (pH = 2.6); Vegetation downgradient of the seep was blackened and dead, likely indicating that low pH of the seep waters contributed to the death of adjacent tundra vegetation (Supplementary Fig. 2) and lower pH in receiving stream waters. Further, concentrations of SO_4^{2-} (Fig. 2b) and major (Fe, Al, and manganese (Mn)) and trace elements (Co, Ni, Cu, Zn, Cd, lead (Pb), arsenic (As)) were 1–2 orders of magnitude higher in orange streams relative to reference streams across the three evaluated watersheds (Fig. 2c, d, Supplementary Fig. 1), and highly elevated in the terrestrial seep in the Agashashok River. For instance, total Zn and Ni concentrations were 16 and 43 times higher in impaired reaches ($n = 8$) compared to reference streams ($n = 10$) and as high as 340 mg L^{-1} and 5.4 mg L^{-1} in the terrestrial seep, respectively. Concentrations of filtered and particulate metals of orange streams show that nearly 90% of the total metal content is particulate, with one exception being notable concentrations of dissolved aluminum (Al; Supplementary Fig. 1)²⁰.

Constraining the onset of stream discoloration

To discern the onset of stream discoloration, we focused on Fe-impacted streams from the three watersheds we sampled to determine the chemical composition of the impaired water: the Agashashok, Kugururok, and Salmon rivers. Using Landsat images from the mid-1980s through 2022, we calculated a Redness Index that detects the red color of Fe oxides based on a comparison of spectral bands (see "Methods" for details)²². Landsat analyses

Fig. 2 | Summary of geochemical observations from impaired orange streams and unimpaired reference sites. Box plots of (a) pH, (b) SO_4^{2-} , and (c) sum of total metals (Al, Mn, Fe, Zn, Ni, Cu, Co, Cd, As, Pb) of unimpaired streams ($n = 13$) and impaired streams ($n = 10$) of the Agashashok, Kugururok, and Salmon rivers, and a terrestrial seep ($n = 1$). **d** Pie chart indicating average distribution of metals from unfiltered water samples of impaired streams. Box plots present the median as the center line, the 75th and 25th percentile ranges as the upper and lower box boundaries, the 90th and 10th percentiles are the error bars, and letters identify differences of statistical significance (two-tailed t tests: pH: $t = 2.51$, $df = 20$, $P = 0.035$; SO_4^{2-} : $t = -2.777$, $df = 15$, $P = 0.014$; Sum of Metals: $t = -3.353$, $df = 15$, $P = 0.004$).



indicated elevated redness in these streams in 2018 (Fig. 3). We also observed elevated Redness Index values (>1.5) during 2007–2008 in the Salmon River. Review of high-resolution IKONOS imagery (<5 m) indicates impacted conditions in 2008–2010, 2012, and 2018 at seeps in some headwater tributaries of the Salmon River (Supplementary Table 1). However, annual Landsat scenes (30 m) downstream suggest a possible shift from orange to clearwater conditions on the mainstem Salmon River from 2008 to 2018 (Fig. 2). Additional research could improve understanding of the onset, duration, seasonality, and underlying causes of downstream impacts.

Biological consequences of trace metal mobilization

Arctic rivers provide habitat for a broad array of resident and diadromous fish (i.e., fish that migrate between salt and fresh water), many of which are critical for subsistence, sport, and commercial fisheries. Climate change is already impacting high-latitude fish species, including Pacific salmon (*Oncorhynchus* spp.), due to effects of warming on marine and freshwater ecosystems^{23–25}. Adding to those concerns, mobilization of Fe and toxic metals to Arctic streams in northern Alaska may both degrade water quality and reduce habitat. Within Kobuk Valley National Park, a considerable decrease in stream biodiversity was observed at an existing monitoring location when a headwater tributary of the Akillik River changed from clear to orange between early and late summer of the same year (Fig. 4; Supplementary Fig. 3). Here, we documented the complete loss of fish species, juvenile Dolly Varden (*Salvelinus malma*) and Slimy Sculpin (*Cottus cognatus*)²⁶ subsequent to abrupt decreases in stream pH (Supplementary Fig. 3). The impact on both the small-bodied sculpin with a small home range²⁷ and the wide-ranging Dolly Varden with either an amphidromous or resident life history strategy²⁸ suggests the broad effect of the shift in water quality. The loss of fish coincided with a steep decrease in benthic macroinvertebrate diversity and periphyton biomass²⁹. The exact mechanisms driving these biological shifts are currently unresolved but likely occurred through several pathways (Fig. 5). First, elevated concentrations of toxic metals (e.g., Fe, Zn, Ni, Cu, Cd) can be directly absorbed from the water column by aquatic biota, yielding direct toxic effects on producers and

consumers. The accumulation of these metals in fish gills, liver, and muscle tissue is known to structurally impair gills, damage DNA, and decrease growth and survival^{19,30}. Ultimately, a complete water quality assessment could ascertain if trace metal concentrations exceeded acute and chronic exposure levels for a range of aquatic biota based on water pH, hardness, and DOC concentration^{31,32}.

In a second pathway, the presence of Fe(III) precipitates and subsequent deposition on benthic surfaces may negatively affect lower trophic levels, either by blanketing benthic habitat or through the bioaccumulation of metals at higher trophic levels (Fig. 5). The blanketing of benthic habitat by metal oxides, and in particular both Fe and Mn oxides, may contribute to enhanced trace metal sorption and uptake³³ and subsequent incorporation into the food web. A third pathway reducing fish abundance may occur through the emigration of fish to unimpaired habitat. Beyond the deleterious effects when elevated, Fe concentrations may decrease to levels that produce a positive effect on food web productivity by fertilizing these oligotrophic ecosystems. For instance, nitrogen-fixing primary producers that are Fe-limited respond positively to higher concentrations, with bottom-up effects through the food web³⁴. Other metals may also have positive effects on stream biota, such as molybdenum limitation of nitrogen fixation and nitrate reduction³⁵. Thawing permafrost may also increase the flux of Fe to the Arctic Ocean, where Fe may function to stimulate marine phytoplankton productivity³⁶. Ultimately, the consequences of this recent metal mobilization for stream food webs are uncertain in Arctic watersheds undergoing permafrost thaw.

Possible causes of trace metal mobilization to streams

The thawing of permafrost can alter stream chemistry through changes in watershed hydrology and biogeochemical cycling in the Arctic. Permafrost restricts water infiltration, confining groundwater movement to shallow soil horizons⁸. Permafrost thaw allows deeper groundwater penetration and alteration of stream flows, temperature, and chemistry^{7,37,38}. Because permafrost stores large amounts of carbon, nutrients, and trace metals, often for hundreds to thousands of years^{2–4}, its thaw transfers soil organic matter and

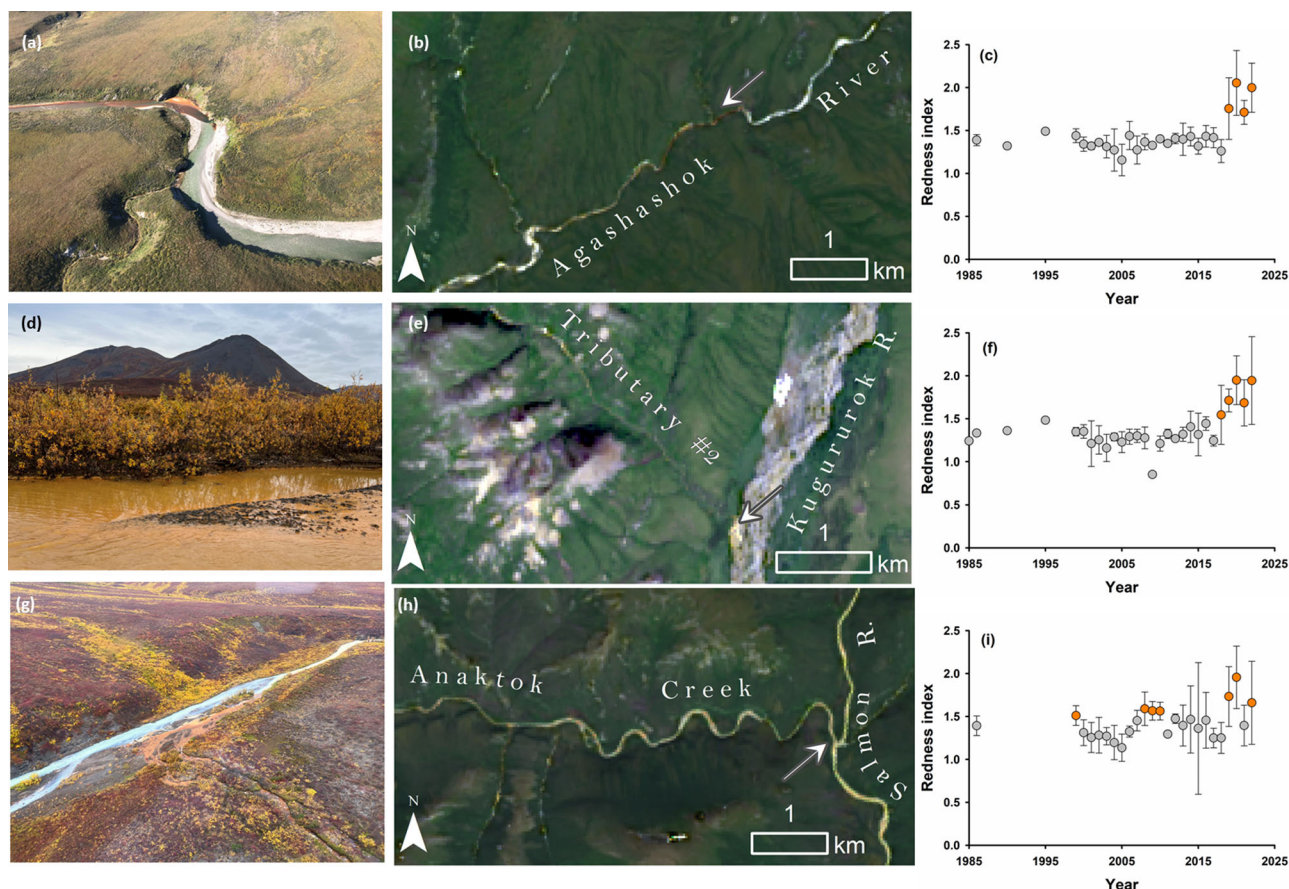


Fig. 3 | Time-series analysis of three discolored streams in northwest Alaska using Landsat. Field photographs (a, d, g), Landsat satellite images (b, e, h), and time-series data for an optical reflectance index, or Redness Index (c, f, i), for the Agashashok River (top row), a tributary of the Kugururuk River (middle row), and the Anaktok Creek tributary of the Salmon River (bottom row) in northwest Alaska. The

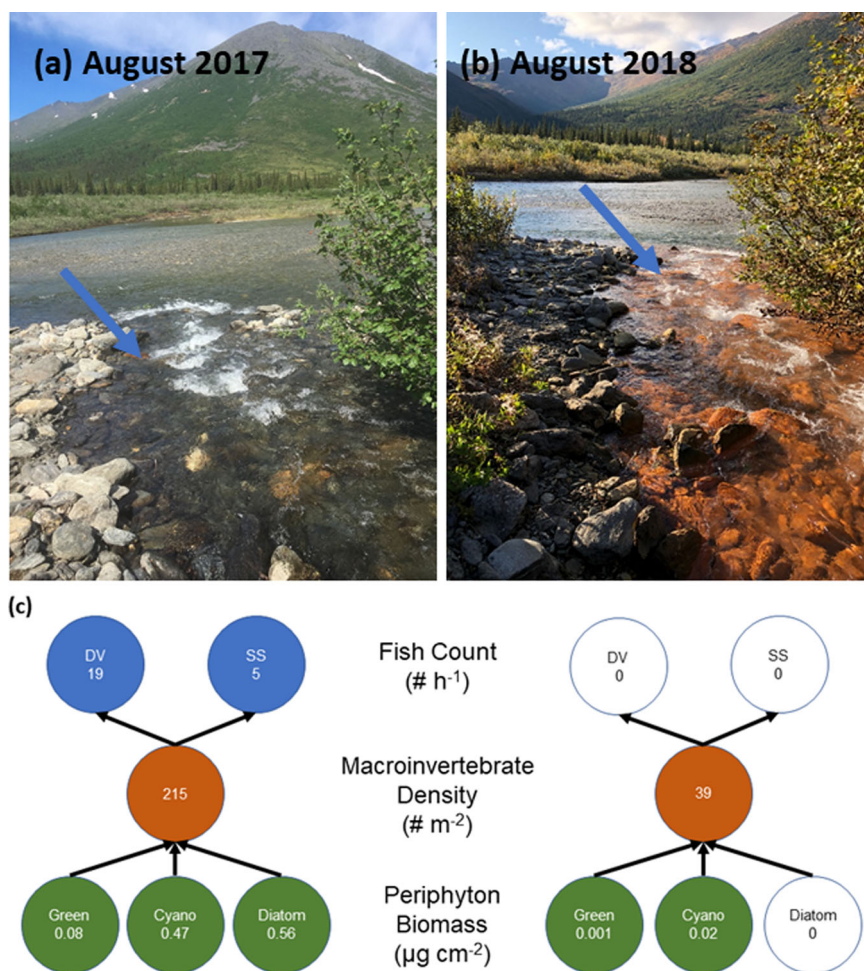
time-series data were generated using average Redness index values (see methods for details) for summer months of each year from 1985 through 2022. The orange circles indicate Redness Index values > 1.5, discolored by Fe mobilization. Gray circles represent Redness Index values < 1.5, indicating clear water or streams unimpacted by Fe mobilization. Photo credits Jonathan O'Donnell/NPS; Michael Carey/USGS.

mineral deposits from a perennially frozen and largely inert state to a biogeochemically active state. The altered soil saturation, groundwater flow, and warmer soil temperatures enhance microbial and weathering processes, which can change the chemistry of groundwater inputs to streams. In recent years at meteorological stations located in each of the watersheds, air and ground temperatures have abruptly increased compared to the preceding 30-year record, exceeding the freezing threshold for near-surface permafrost³⁹. Shrubification and associated increases in snowpack in the region can also contribute to permafrost thaw⁴⁰. Given the coincidence of warm, snowy years in 2018 and 2019 with elevated Redness index for the three sampled watersheds (Supplementary Fig. 4), we hypothesize that climate change-induced permafrost thaw is responsible for the abrupt shifts in stream color and chemistry. Important changes include shifts in the concentration, age, and character of dissolved organic matter⁴¹ and the flux of dissolved nitrogen species, base cations, trace metals, SO_4^{2-} , and suspended sediments^{67,17}. Permafrost thaw has already been linked to dramatic shifts in water quality in Arctic national parks⁴², including increased SO_4^{2-} and Fe concentrations and decreased pH (to <3)⁴³, which may be in response to changes in chemical weathering of minerals. Further, not all permafrost is the same composition. Soil parent material, geologic setting, and ground ice content all influence stream chemistry in Arctic watersheds⁴².

We propose two distinct processes that may explain orange streams and are end member processes along a continuum of combined effects (Fig. 5). The chemistry of orange streams, including the lower pH and relatively high concentrations of SO_4^{2-} and trace metals, is consistent with sulfide mineral weathering as the primary driver of stream discoloration. In upland terrain, permafrost thaw can expose mineral deposits, or more

commonly, sulfide-rich rocks such as shales and their metamorphosed equivalents, to chemical weathering processes, altering the geochemistry of groundwater and receiving stream water (Hypothesis 1 [H1]⁹; Upland Processes panel in Fig. 5). Importantly, while Alaska has an extensive mining history, our observations of orange streams are not downstream of any mines and are mostly within protected lands. Similar findings have also been documented near Red Dog Mine in northwest Alaska, where thermal erosional features have caused abrupt increases in stream total dissolved solids, which are comprised mainly of SO_4^{2-} , calcium (Ca^{2+}), Fe, and diverse trace metals⁴³. The Brooks Range hosts extensive sulfide minerals, including pyrite (FeS_2)⁴⁴, the most abundant, which can undergo enhanced oxidative weathering in association with thawing permafrost and enhanced groundwater flows⁹. Pyrite weathering releases Fe^{2+} and sulfuric acid (H_2SO_4) to groundwater and often results in concomitant release of trace metals hosted in the pyrite that can be toxic to aquatic organisms (e.g., zinc (Zn), nickel (Ni), copper (Cu), cadmium (Cd)). Additional metal sulfide minerals might also be present and vulnerable to oxidative weathering. Following mobilization and groundwater transport to surface water, Fe^{2+} will oxidize to Fe^{3+} and form Fe(III) oxyhydroxide minerals under circumneutral pH. Regardless of the oxidation state of Fe released to rivers, which was not confirmed in this study, Fe-oxyhydroxides will form at the pH of mainstem rivers. The precipitation of Fe(III) oxyhydroxide is likely a major source of increased turbidity in orange streams, with important implications for stream biota⁴⁵. The susceptibility of streams to metal inputs from chemical weathering of sulfide minerals (H1) and the ultimate fate of Fe and other metals will be influenced by carbonate lithologies, which are common in the Brooks Range⁴⁶ and buffer acidic groundwater inputs to

Fig. 4 | Tracking the effects of iron mobilization on stream food webs. Images of a headwater tributary of the Akillik River in Kobuk Valley National Park, Alaska, illustrating a shift from clearwater on June 12, 2017 (a) to orange stream conditions on August 30, 2018 (b). The blue arrows point to the same boulder near the confluence. c Stream food web data collected in before (September 2017) and after (September 2018) the color change demonstrates the reduction in benthic biofilm production, corresponding decline in benthic macroinvertebrate density, and a complete loss of resident fish (DV = Dolly Varden, SS = Slimy Sculpin). The open white circles in (c) represent observations where species absence was documented.



streams. Increases in pH can also result from mixing with other waters with substantially higher pH, such as through the convergence of a tributary with a larger stream. Importantly, some metals such as Fe will precipitate from solution once O₂ and pH levels rise, while others can remain in solution over long distances of transport under more typical surface water conditions.

Climate change is dramatically reducing the spatial extent of Earth's cryosphere, with extensive consequences for surface waters⁶⁷. This study is the first to report acid rock drainage in response to permafrost thaw in an Arctic region unimpacted by land-use effects. Prior research has reported acid rock drainage in subarctic and Arctic regions; however, these studies showed how road construction accelerated active layer thickening and subsequent water quality impacts⁴⁷. In an analogous situation to our observations in the Brooks Range, natural acid rock drainage has increased in the temperate zone of Europe and South America. There, climate change, drought, and soil thermal shifts have facilitated enhanced sulfide mineral oxidation, with acid rock drainage tracking the elevation shift in mountain permafrost and periglacial limits^{48,49}. For instance, in the European Alps, acid rock drainage was associated with warmer soil temperatures and enhance groundwater flow in a regions underlain by mountain permafrost and pyrite-bearing rock^{50,51}. Taken together, the preliminary observations of sulfide mineral weathering being a primary process driving the increase metal loading in northwest Alaskan rivers is consistent with processes observed globally.

Alternatively, in lowland organic-rich permafrost soils (e.g., peatlands) and mineral-soil wetlands, changes in soil drainage and redox potential due to soil thaw can mobilize and transform stored Fe and carbon through coupled microbially facilitated reactions (e.g., Fe reducing bacteria), enhancing lateral transport to streams (Hypothesis 2 [H2]; Lowland Processes panel in Fig. 5)^{10,13}. Permafrost thaw can cause both wetting and

drying of soils, depending on topographic factors, ground ice content, soil texture, and new groundwater flow patterns⁵². In peatlands and other lowland ecosystems, permafrost thaw often reduces soil drainage, causing soils to become water-logged. Under these conditions, for example, Fe(III) associated with soil organic carbon can undergo dissimilatory iron reduction by heterotrophic microbes at circumneutral pH to mobilize dissolved Fe²⁺ ions. In this form under anoxic soil conditions, Fe²⁺ can then be transported by groundwater to streams, where Fe²⁺ will oxidized to Fe³⁺ and form Fe(III) oxyhydroxide particulates in surface water. Surface water pH is a master variable on the Fe²⁺ oxidation rate and Fe³⁺ solubility in surface waters. Under H2, we are less likely to observe elevated SO₄²⁻ and trace metals associated with elevated Fe concentrations in orange streams compared to H1, which gives us an effective way of distinguishing which process may be responsible for stream water impairment in a given catchment. Mechanisms described in H1 and H2 may also co-occur at an impaired site. While H1 appears to be the primary driver of orange streams in mountainous upland terrain of Arctic national parklands, further work is needed to partition the relative importance of both mechanisms in Arctic river networks draining lowland terrain.

Considerable uncertainty exists regarding the subsurface flow paths in thawing permafrost terrain that contribute to metal transport to streams. Our observations of orange streams indicate both point and non-point sources of Fe to stream ecosystems, potentially reflecting different modes of permafrost thaw⁵³. Point sources may be driven by localized permafrost thaw, which can allow for new flow paths to wet sulfide-bearing minerals. Abrupt deep thaw may also increase permeability of aquifers, either through the loss of excess ice and increased hydraulic conductivity⁸ or through altered groundwater flux along geologic fault lines⁵⁴. As permafrost thaws, deep sub-permafrost groundwater may recirculate, contributing water,

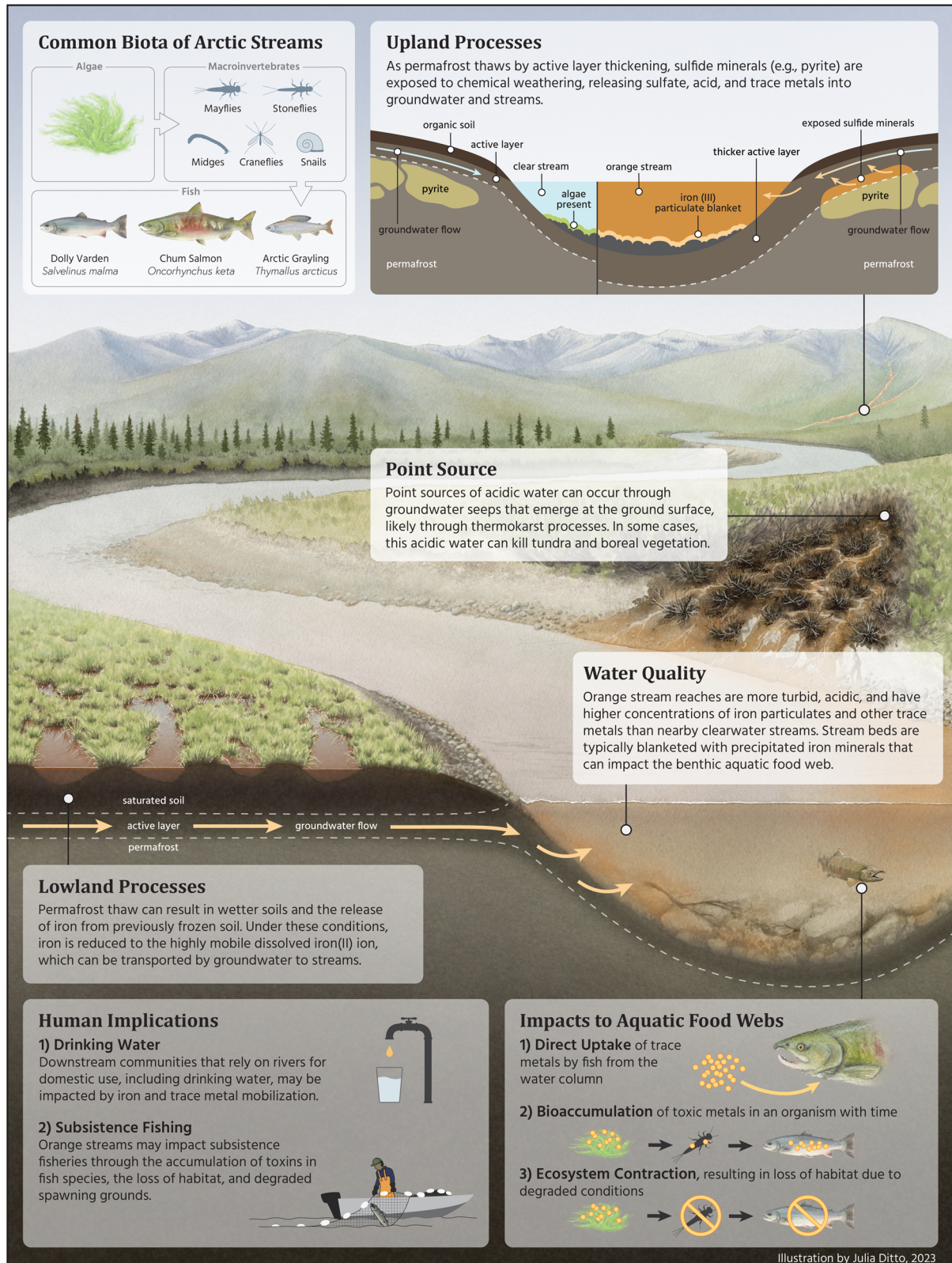


Fig. 5 | Conceptual models of hypothesized processes contributing to the discoloration of Arctic streams in Alaska’s Brooks Range. The illustration includes consequences for water quality, aquatic food webs, and human implications, including drinking water and subsistence fishing.

solutes, and other metals to stream flow. Non-point sources are more likely caused by broad-scale deepening of the active layer and talik formation (perennial unfrozen layers)⁵⁵. Under this scenario, groundwater is routed primarily through comparatively shallow supra-permafrost zones where Fe is mobilized through chemical weathering (H1) or microbial processes (H2).

Implications for rural communities and subsistence users

The emergence of orange streams in northern Alaska represents an unexpected threat to subsistence fisheries and rural drinking water supplies. Communities in northwest Alaska are disconnected by roads and depend both socioeconomically and culturally on subsistence foods such as fish,

large ungulates, and marine mammals⁵⁶. Our preliminary data suggest that metal mobilization may increase the vulnerability of important subsistence fish species—such as Dolly Varden, chum salmon (*Oncorhynchus keta*), and whitefish (*Coregonus* sp.)—to population decline. The scale of these impacts may depend on the timing and magnitude of metal inputs and their downstream persistence, most importantly the metal speciation under oxygenated, circumneutral pH conditions (i.e., dissolved versus particulate) and other water quality conditions (e.g., hardness and DOC concentration).

Beyond the effects on subsistence resources, the metals transported downstream from headwater streams to higher-order rivers may impact drinking water supplies to rural communities. Preliminary measurements indicate that As and Pb concentrations did not exceed U.S. EPA drinking water criteria in the impaired reaches tested, though concentrations of Cd, Ni, and Mn exceeded either U.S. EPA drinking water criteria or World Health Organization guidelines (Supplementary Fig. 1)^{31,32}. At a minimum, this disturbance may present taste issues for drinking water that require enhanced water filtration to mitigate the increased particulate load. In rural Alaska, climate and associated disturbances (permafrost thaw) can function as primary drivers of water resource impairment. Disturbance along river corridors, including bank erosion and retrogressive thaw slumps, can profoundly affect water quality through deposition of sediments, nutrients, and ions in river water⁵⁷. The observed presence of dissolved and precipitated metals through processes described here present a similar challenge to drinking water access in remote Alaska, particularly for villages proximal to orange streams.

One community, the coastal village of Kivalina near Cape Krusenstern National Monument (Fig. 1), is particularly vulnerable to drinking water impairment. The community relies on drinking water primarily from the Wulik River, which drains National Park lands but is also downstream from the Red Dog Mine (Fig. 1). Permafrost thaw combined with high flows have altered sediment loads in the Wulik River watershed, affecting the drinking water supply in Kivalina⁵⁸. In some instances, bottled water has been shipped to residents of Kivalina during periods of impaired river water. Similar issues have impacted the village of Selawik, located south of Kobuk Valley National Park and downstream of a large permafrost thaw slump depositing silt into the Selawik River and impacting drinking water supplies for the village⁵⁹. Recent metal mobilization poses an additional threat in the face of all these challenges.

The recent onset of stream discoloration in Alaska's Brooks Range is an emergent threat to stream ecosystems, water quality, and subsistence resources in Arctic Alaska and potentially other regions undergoing permafrost thaw. Climate change and associated permafrost thaw appear to be the primary drivers of stream impairment, as shifts in stream color coincide with a period of rapid warming and increased snowfall. Our initial findings indicate that orange streams are an indicator of impaired water quality and are associated with declines in stream biodiversity and habitat degradation (as outlined in Fig. 5). Understanding the magnitude, spatial extent, persistence, and timing of stream degradation may inform management responses by federal and state agencies and adaptation by rural communities and subsistence users.

Methods

Geochemical assessment of impaired and reference streams

We compared the chemical composition of orange streams to nearby unimpaired reference streams, largely derived from the NPS Arctic Inventory & Monitoring Program^{20,42}. All stream and river water samples were collected during the open-water period between June and September in 2022²⁰. At sites within the watersheds of the Agashashok, Kugururok, and Salmon rivers, water samples from discolored reaches and reference locations were collected 25 cm below the surface or shallower in streams less than 25 cm deep in a well-mixed location of the stream reach and were filtered in situ using a 0.45- μ m high-capacity capsule filter connected to a Geopump Series II peristaltic pump (Geotech Environmental Equipment, Inc. Denver, CO, USA). Discrete in situ measurements of stream temperature, pH, specific conductivity, and dissolved oxygen were collected

using a YSI ProDSS multiparameter meter (YSI Incorporated, Yellow Springs, OH, USA). Continuous in situ measurements were also collected by deploying a YSI EXO3 multiparameter sonde. Samples for metal analysis were preserved in the field with 1% volume/volume Omnitrace HNO₃ and stored at 4 °C until analysis. Total metal concentrations on unfiltered water samples were measured after digestion (3% HNO₃, 8 hour digest at 65 °C) and matrix adjustment (to 2% HNO₃, 0.5% HCl) by ICP-MS analysis (ThermoFisher iCAP RQ ICP-MS)⁴⁹. Filtered metal concentration was measured by ICP-MS analysis⁶⁰. Samples for sulfate were stored at 4 °C and analyzed by ion chromatography (Metrohm A Supp 7 column)⁶¹.

Time series of stream discoloration using Landsat

Time series of historical water conditions were produced from Landsat, Collection 2, Tier 1 Surface Reflectance products derived by the USGS (Fig. 3)^{22,62}. Surface reflectance improved the comparison between multiple images over the same region by accounting for atmospheric effects such as aerosol scattering and thin clouds, which assisted in the detection and characterization of Earth surface change. Areas of interest (AOIs) within study rivers were manually delimited to correspond with Landsat pixel geometry and observed Fe precipitate in surface water and orange staining on stream beds. AOI area ranges from 0.5 to 1.0 hectare. From all available Landsat scenes acquired between 1985 and 2022, we filtered and retained only scenes acquired over the AOI for the months of July or August to avoid turbidity effects from breakup and vegetation senescence, and with scene-wide cloud cover <30%. Clouds and cloud shadows were masked from the resultant scenes.

A ferric iron Redness Index was calculated⁶³ for each scene based on the ratio of surface reflectance sensed in the red band and blue band⁶⁴. The Redness Index is sensitive to iron at low concentrations⁶³ and is fitting for detecting the presence of ferric iron minerals (e.g., hematite, goethite, and jarosite) which present as shades of red and orange and strongly affect the Landsat blue band⁶⁵. In general, clearwater streams with low DOC concentrations¹⁶ and high pH may be more vulnerable to orange discoloration, as opposed to brown-water streams with higher DOC and lower pH⁴². Available daily values from July and August and average values were plotted, and outlier values were inspected and removed from analysis following manual scene inspection for atmospheric contaminants missed in the masking process (e.g., smoke from summer wildfires). For scenes acquired by Thematic Mapper sensors (Landsat 4 and 5) and the Enhanced Thematic Mapper (ETM+) sensor (Landsat 7), a simple ratio of [Red/Blue] was calculated. For scenes acquired by the Operational Land Imager (OLI) sensor (Landsat 8 and 9), we included a site-specific corrective factor [e.g. (Red / Blue) - X, where X is the correction factor] so values were consistent with the previous sensors. Mean Redness Index values were calculated from all pixels intersected by the area of interest for each Landsat scene. Site-specific corrective factors are calculated by comparing mean annual Redness Index values derived from ETM+ and OLI sensors for the years (2013–2022) when both sensors are in operation. The average offset is calculated from all available years and applied to individual OLI scenes. Finally, a mean annual Redness Index value was summarized from available values for each year and graphed. For the overall study area, mean annual Redness Index values ranged from 0 to +2.5. We did not directly compare iron concentration in surface water with Redness Index values. We also assumed consistent surface conditions, given that stream channels in our AOIs were incised and not meandering or braided in these sections of the watershed. Waters are historically clear flowing from non-glacial sources. Assuming the AOI corresponds with a consistent water surface, values of 0–0.5 were interpreted as deep clear water, 0.5–1.5 as clear shallow water, and >1.5 as Fe oxide-stained water. We identified a Redness Index value of 1.5 as a threshold to identify the timing of stream color change from clear to orange/red. Similar approaches have been used when setting thresholds for index values⁶⁶. The threshold value was supported by (1) field observations of recent stream color change, and (2) derived Redness Index values for control surfaces with no known change (Feniak Lake, Noatak National Preserve; Great Kobuk Sand Dunes, Kobuk Valley National Park).

Stream food web characterization

Benthic biofilm, benthic macroinvertebrates, and resident fish were collected from a tributary of the Akillik River in Kobuk Valley National Park prior to stream discoloration (September 2017) and after stream discoloration (September 2018). We accessed this site via Robinson R44 II helicopter. Benthic biofilm was measured in situ using a Benthotorch (bbe Moldaenke, Kiel, Germany) hand-held fluorometer, which distinguishes taxa (green algae, cyanobacteria, diatoms) and provides estimates of standing biomass. Each tributary was measured at 3 random transects and at each transect, 3 measurements were taken with the Benthotorch near the right bank, in the middle of the thalweg, and near the right bank. The nine biofilm measurements were averaged to characterize the headwater tributary each year and then average across years. Benthic macroinvertebrates were sampled using kick nets. Four kicknet samples were collected in riffles and 4 kicknet samples collected in runs per headwater stream with collection lasting 1 minute per sample and encompassing 0.25 m² area (National Aquatic Monitoring Center, namc-usu.org). In the laboratory, individuals were identified to the lowest practical taxonomic level (usually Family) to compare composition, richness, and density. Macroinvertebrate samples were processed by the National Aquatic Monitoring Center (Logan, UT, USA) and data are publicly available²⁹. Resident fish were collected using backpack electrofishing. Upon capture, fish were identified to species.

Reporting summary

Further information on research design is available in the Nature Portfolio Reporting Summary linked to this article.

Data availability

The data that support the findings of this study are publicly available through the U.S. Geological Survey^{20–22,26,29}. Data releases are available for geochemistry (<https://alaska.usgs.gov/products/data.php?dataid=611>; <https://alaska.usgs.gov/products/data.php?dataid=401>), remote sensing analyses (<https://alaska.usgs.gov/products/data.php?dataid=642>), resident fish (<https://alaska.usgs.gov/products/data.php?dataid=598>), and stream macroinvertebrates (<https://alaska.usgs.gov/products/data.php?dataid=643>).

Received: 13 September 2023; Accepted: 10 May 2024;

Published online: 20 May 2024

References

- Kendrick, M. R. et al. Linking permafrost thaw to shifting biogeochemistry and food web resources in an arctic river. *Glob Change Biol.* **24**, 5738–5750 (2018).
- Hugelius, G. et al. Estimated stocks of circumpolar permafrost carbon with quantified uncertainty ranges and identified data gaps. *Biogeosciences* **11**, 6573–6593 (2014).
- Schuster, P. F. et al. Permafrost stores a globally significant amount of mercury. *Geophys. Res. Lett.* **45**, 1463–1471 (2018).
- Strauss, J. et al. A globally relevant stock of soil nitrogen in the Yedoma permafrost domain. *Nat. Comm.* **13**, 6074 (2022).
- Smith, S. L., O'Neill, H. B., Isaksen, K., Noetzli, J. & Romanovsky, V. E. The changing thermal state of permafrost. *Nat. Rev. Earth Environ.* **3**, 10–23 (2022).
- Frey, K. E. & McClelland, J. W. Impacts of permafrost degradation on arctic river biogeochemistry. *Hydrol Process* **23**, 169–182 (2009).
- Toohey, R. C. et al. Multidecadal increases in the Yukon River Basin of chemical fluxes as indicators of changing flowpaths, groundwater, and permafrost. *Geophys. Res. Lett.* **43**, 12120–12130 (2016).
- Walvoord, M. A. & Kurylyk, B. L. Hydrologic impacts of thawing permafrost – A review. *Vadose Zone J.* **15**, <https://doi.org/10.2136/vzj2016.01.0010> (2016).
- Zolkos, S., Tank, S. E. & Kokelj, S. V. Mineral weathering and the permafrost carbon-climate feedback. *Geophys. Res. Lett.* **45**, 9623–9632 (2018).
- Patzner, M. S. et al. Iron mineral dissolution releases iron and associated organic carbon during permafrost thaw. *Nat. Comm.* **11**, 6329 (2020).
- O'Donnell, J. A., Douglas T., Barker, A., & Guo, L. Changing biogeochemical cycles of organic carbon, nitrogen, phosphorus, and trace elements in Arctic rivers in *Arctic Hydrology, Permafrost and Ecosystems* (ed. Yang D., & Kane, D. L.) 315–348 (Springer, 2021).
- Vonk, J. E. et al. Reviews and syntheses: Effects of permafrost thaw on Arctic aquatic ecosystems. *Biogeosciences* **12**, 7129–7167 (2015).
- Barker, A. J. et al. Iron oxidation-reduction processes in warming permafrost soils and surface waters expose a seasonally rustic arctic watershed. *ACS Earth Space Chem.* **7**, 1479–1495 (2023).
- Hirst, C. et al. Seasonal changes in hydrology and permafrost degradation control mineral element-bound DOC transport from permafrost soils to streams. *Glob. Biogeochem. Cy.* **36**, <https://doi.org/10.1029/2021GB007105> (2022).
- Miner, K. R. et al. Emergent biogeochemical risks from Arctic permafrost degradation. *Nat. Clim. Change* **11**, 809–819 (2021).
- Pokrovsky, O. S. & Schott, J. Iron colloids/organic matter associated transport of major and trace elements in small boreal rivers and their estuaries. *Chem. Geol.* **19**, 141–179 (2002).
- Kemeny, P. C. et al. Arctic permafrost thawing enhances sulfide oxidation. *Glob. Biogeochem. Cy.* **37**, <https://doi.org/10.1029/2022GB007644> (2023).
- Sullivan, P. F., O'Donnell, J. A., Dial, R. & Hewitt, R. Opinion: the degradation of a wild and scenic river in Alaska's Brooks Range. *Anchorage Daily News* <https://www.adn.com/opinions/2022/11/15/opinion-the-degradation-of-a-wild-and-scenic-river-in-alaskas-brooks-range/> (2022).
- Dos Santos Vergilio, C. et al. Immediate and long-term impacts of one of the worst mining tailing dam failure worldwide. *Sci. Tot. Environ.* **756**, 143697 (2021).
- Koch, J. C., Poulin, B. A., O'Donnell, J. A. & Carey, M. P. Chemistry of orange streams in Northwestern Alaska, 2022. *U.S. Geological Survey data release* <https://doi.org/10.5066/P9DZSQ43> (2023).
- O'Donnell, J. A., Koch, J. C., Carey, M. P., & Poulin, B. A. Stream and river chemistry in watersheds of northwestern Alaska, 2015–2019. *U. S. Geological Survey data release* <https://doi.org/10.5066/P9SBK2DZ> (2021).
- Baughman, C. A. Time series analysis of metal mobilization in select Arctic streams in Alaska. *U.S. Geological Survey data release* <https://doi.org/10.5066/P9TP9TZH> (2023).
- Fossheim, M. et al. Recent warming leads to a rapid borealization of fish communities in the Arctic. *Nat. Clim. Change* **5**, 673–677 (2015).
- Carey, M. P. et al. Egg retention of high-latitude sockeye salmon (*Onchorhynchus nerka*) in the Pilgrim River, Alaska, during the Pacific marine heatwave of 2014–2016. *Polar Biol.* **44**, 1643–1654 (2021).
- Von Biela, V. R. et al. Premature mortality observations among Alaska's Pacific salmon during record heat and drought in 2019. *Fisheries* **47**, 157–168 (2022).
- Carey, M. P., Koch, J. C., O'Donnell, J. A. & Riddle-Berntsen, A. E. Length, weight, energy density, and isotopic values of fish from rivers in Northwest Alaska, 2015–2019. *U.S. Geological Survey data release* <https://doi.org/10.5066/P9WGRX66> (2023).
- Gray, M. A., Curry, R. A., Arciszewski, T. J., Munkittrick, K. R. & Brasfield, S. M. The biology and ecology of slimy sculpin: A recipe for effective environmental monitoring. *FACETS* **3**, 103–127 (2018).
- Carey, M. P., von Biela, V. R., Brown, R. J. & Zimmerman, C. E. Migration strategies supporting salmonids in Arctic Rivers: A case study of Arctic Cisco and Dolly Varden. *Animal Migration* **8**, 132–143 (2021).
- Carey, M. P., Koch, J. C., O'Donnell, J. A., & Riddle-Berntsen, A. E. Macroinvertebrates from Rivers in Northwest Alaska, 2015–2019. *U.S. Geological Survey data release* <https://doi.org/10.5066/P90B3Q00> (2023).

30. Egnew, N. et al. Physio-biochemical, metabolic nitrogen excretion and ion-regulatory assessment in largemouth Bass (*Micropterus salmoides*) following exposure to high environmental iron. *Ecotox Env. Safety* **208**, 111526 (2021).
31. U.S. Environmental Protection Agency. National recommended water quality criteria – Aquatic life criteria table. <https://www.epa.gov/wqc/national-recommended-water-quality-criteria-aquatic-life-criteria-table> (2024).
32. World Health Organization. Guidelines for drinking-water quality: fourth edition incorporating the first and second addenda. Geneva: World Health Organization; Licence: CC BY-NC-SA 3.0 IGO (2022).
33. Fuller, C. C. & Harvey, J. W. Reactive uptake of trace metals in the hyporheic zone of a mining-contaminated stream, Pinal Creek, Arizona. *Environ. Sci. Technol.* **34**, 1150–1155 (2000).
34. Larson, C. A., Mirza, B., Rodrigues, J. L. M. & Passy, S. I. Iron limitation effects on nitrogen-fixing organisms with possible implications for cyanobacterial blooms. *FEMS Microbiol Ecol.* **94**, <https://doi.org/10.1093/femsec/fiy046> (2018).
35. Glass, J. B., Axler, R. P., Chandra, S., & Goldman, C. R. Molybdenum limitation of microbial nitrogen assimilation in aquatic ecosystems and pure cultures. *Fron. Microbial.* **13**, <https://doi.org/10.3389/fmicb.2012.00331>.
36. Terhaar, J., Lauerwald, R., Regnier, P., Gruber, N., & Bopp, L. Around one third of current Arctic Ocean primary production sustained by rivers and coastal erosion. *Nat. Comm.* **12**, <https://doi.org/10.1038/s41467-020-20470-z> (2021).
37. Sjöberg, Y. et al. Permafrost promotes shallow groundwater flow and warmer headwater streams. *Water Res. Res.* **57**, <https://doi.org/10.1029/2020WR027463> (2020).
38. Koch, J. C. et al. Sensitivity of headwater streamflow to thawing permafrost and vegetation change in a warming Arctic. *Environ. Res. Lett.* **17**, 044074, <https://doi.org/10.1088/1748-9326/ac5f2d> (2022).
39. Swanson, D. K., Sousanes, P. J., & Hill, K. Increased mean annual temperatures in 2014–2019 indicate permafrost thaw in Alaskan national parks. *Arct. Antarct. Alp. Res.* **53**, 1–19 (2021).
40. Jafarov, E. E. et al. Modeling the role of preferential snow accumulation through talik development and hillslope groundwater flow in a transitional permafrost landscape. *Env. Res. Lett.* **13**, <https://doi.org/10.1088/1748-9326/aadd30>.
41. Spencer, R. G. M. et al. Detecting the signature of permafrost thaw in Arctic rivers. *Geophys. Res. Lett.* **42**, 2830–2835 (2015).
42. O'Donnell, J. A. et al. Dissolved organic matter composition of arctic rivers: Linking permafrost and parent material to riverine carbon. *Glob. Biogeochem. Cy.* **30**, 1811–1826 (2016).
43. Clawson, C. M. Aquatic biomonitoring at Red Dog Mine, 2021. Alaska Department of Fish & Game, Technical Report No. 22-01, https://www.adfg.alaska.gov/static/home/library/pdfs/habitat/23_02.pdf (2022).
44. Moore, D. W., Young, L. E., Modene, J. S. & Plahuta, J. T. Geologic setting and genesis of the Red Dog zinc-lead-silver deposit, western Brooks Range. *Alaska. Econ. Geol.* **81**, 1696–1727 (1986).
45. Vuori, K.-M. Direct and indirect effects of iron on river ecosystems. *Annales Zoologici Fennici* **32**, 317–329 (1995).
46. Wilson, F. H., Hults, C. P., Mull, C. G. & Karl, S. M. Geologic map of Alaska. *U.S. Geological Survey Scientific Investigations Map*, **3340**, <https://doi.org/10.3133/sim3340> (2015).
47. Lacell, D., Doucet, A., Clark, I. D. & Lauriol, B. Acid drainage generation and seasonal recycling in disturbed permafrost near Eagle Plains, northern Yukon Territory. *Canada. Chem. Geol.* **242**, 157–177 (2007).
48. Zarroca, M., Roque, C., Linares, R., Salminci, J. G. & Gutierrez F. Natural acid rock drainage in alpine catchments: a side effect of climate warming. *Sci. Tot. Environ.* **778**, <https://doi.org/10.1016/j.scitotenv.2021.146070> (2021).
49. Santofimia, E. et al. Acid rock drainage in Nevado Pastoruri glacier area (Huascaran National Park, Peru): hydrochemical and mineralogical characterization and associated environmental implications. *Environ. Sci. Poll. Res.* **24**, 25243–25259 (2017).
50. Ilyashuk, B. P., Ilyashuk, E. A., Psenner, R., Tessadri, R. & Koinig, K. A. Rock glaciers in crystalline catchments: Hidden permafrost-related threats to alpine headwater lakes. *Glob. Change. Biol.* **24**, 1548–1562 (2018).
51. Wanner, C. et al. Rock glaciers in the Central Eastern Alps – How permafrost degradation can cause acid rock drainage, mobilization of toxic elements, and formation of basuminite. *Glob. Planet. Change* **227**, 104180 (2023).
52. Jorgenson, M. T. et al. Reorganization of vegetation, hydrology and soil carbon after permafrost degradation across heterogeneous boreal landscapes. *Environ. Res. Lett.* **8**, <https://doi.org/10.1088/1748-9326/8/3/035017> (2013).
53. Jorgenson, M. T. & Osterkamp, T. E. Response of boreal ecosystems to varying modes of permafrost degradation. *Can. J. Forest Res.* **35**, 2100–2111 (2005).
54. Bense, V. F. et al. Fault zone hydrogeology. *Earth-Sci. Rev.* **127**, 171–192 (2013).
55. Farquharson, L. M., Romanovsky, V. E., Kholodov, A. & Nicolsky, D. Sub-aerial talik formation observed across the discontinuous permafrost zone. *Nat Geosci* **15**, 475–481 (2022).
56. Moerlein, K. J. & Carothers, C. Total environment of change: impacts of climate change and social transitions on subsistence fisheries in northwest Alaska. *Ecol. Soc.* **17**, <https://doi.org/10.5751/ES-04543-170110> (2012).
57. Kokelj, S. V. et al. Thawing of massive ground ice in mega slumps drives increases in stream sediment and solute flux across a range of watershed scales. *J. Geophys. Res-Earth* **118**, 681–692 (2013).
58. Hopkins, K. Lack of drinking water in Kivalina keeps school closed. *Anchorage Daily News* <https://www.adn.com/alaska-news/article/lack-drinking-water-kivalina-keeps-school-closed/2012/08/28/> (2016).
59. DeMarbon, A. Climate change in Arctic Alaska threatens fish stocks, drinking water. *Anchorage Daily News* <https://www.adn.com/rural-alaska/article/climate-change-arctic-alaska-threatens-fish-stocks-drinking-water/2012/06/08/?page=full> (2012).
60. Garbarino, J. R. & Taylor, H. E. An inductively coupled plasma atomic-emission spectrometric method for routine water quality testing. *Appl. Spectrosc.* **33**, 220–226 (1979).
61. Brinton, T. I., Antweiler, R. C., & Taylor, H. E. Method for determination of dissolved chloride, nitrate and sulfate in natural water using ion chromatography. *U.S. Geological Survey Open-File Report*, OFR95-426A (1996).
62. Chen, S. et al. Monitoring temperate forest degradation on Google Earth Engine using Landsat time series analysis. *Remote Sens. Environ.* **265**, 112648 (2021).
63. Rockwell, B. W. Automated mapping of mineral groups and green vegetation from Landsat Thematic Mapper imagery with an example from the San Juan Mountains, Colorado: *U.S. Geological Survey Scientific Investigations Map* 3252, 1 sheet, scale 1:325,000, 25-p. pamphlet, accessed October 10, 2016 at <https://doi.org/10.3133/sim3252> (2013).
64. Abdelsalam, M. G., Stern, R. J. & Berhane, W. G. Mapping gossans in arid regions with Landsat TM and SIR-C images: The Beddaho Alteration Zone in northern Eritrea. *J. African Earth Sci.* **30**, 903–916 (2000).
65. Kokaly, R. F. et al. USGS Spectral Library Version 7: *U.S. Geological Survey Data Series* 1035, 61 p., <https://doi.org/10.3133/ds1035> (2017).
66. Campbell, J. C., & Wynne, R. H. *Introduction to Remote Sensing – Fifth Edition*. 447–448 (Guilford Press, 2011)
67. U.S. Geological Survey. Watershed Boundary Dataset (WBD) <https://www.usgs.gov/national-hydrography/watershed-boundary-dataset> (2023).

68. Gesch et al. *The National Elevation Dataset* <https://www.usgs.gov/publications/national-elevation-dataset> (2018).

Acknowledgements

This work was supported by the U.S. Geological Survey (USGS)-National Park Service (NPS) Water Quality Partnership Program, the USGS Changing Arctic Ecosystem Initiative, and the NPS Arctic Inventory & Monitoring Program. The authors thank all those who contributed observations of orange streams to this effort. The authors also thank Taylor Evinger for analytical support at UC Davis and Julia Ditto for her conceptual diagram illustration (Fig. 3). We also thank the three reviewers, the associate editor and D. Swanson for comments on an earlier version of the manuscript. Any use of trade, firm, or product names is for descriptive purposes only and does not imply endorsement by the U.S. Government.

Author contributions

JAO formulated research goals and aims, curated data, wrote the initial draft and edited subsequent drafts, prepared data visualizations, provided supervision and leadership of research activity, managed and coordinated research activity and execution, acquired funds for the project leading to this publication. MPC formulated research goals and aims, curated data, provided critical review and revision of manuscript drafts, prepared data visualizations, provided supervision and leadership of research activity, managed and coordinated research activity and execution, acquired funds for the project leading to this publication. JCK formulated research goals and aims, curated data, provided critical review and revision of manuscript drafts, provided supervision and leadership of research activity, managed and coordinated research activity and execution, acquired funds for the project leading to this publication. CB developed methodology and conducted formal analysis of remote sensing data, adapted computer code and supporting algorithms to identify impaired streams. KH managed database and prepared a visualization of data and provided a critical review of manuscript drafts. CEZ guided project management, provided oversight, and acquired funds for the project leading to this publication. PFS shared ideas, contributed observations of orange streams, provided water samples from the Salmon River watershed, and provided critical review and revision of manuscript drafts. RD shared ideas, contributed observations of orange streams, and provided critical review and revision of manuscript drafts. TL shared ideas and provided critical review of manuscript drafts. DJC shared ideas and provided critical review of manuscript drafts. BAP formulated research goals and aims, curated data, provided critical review and revision

of manuscript drafts, prepared data visualizations, provided supervision and leadership of research activity, managed, and coordinated research activity and execution, acquired funds for the project leading to this publication.

Competing interests

The authors declare no competing interests.

Additional information

Supplementary information The online version contains supplementary material available at <https://doi.org/10.1038/s43247-024-01446-z>.

Correspondence and requests for materials should be addressed to Jonathan A. O'Donnell.

Peer review information *Communications Earth & Environment* thanks Catherine Hirst and the other, anonymous, reviewer(s) for their contribution to the peer review of this work. Primary Handling Editors: Christophe Kinnard, Clare Davis and Heike Langenberg. A peer review file is available.

Reprints and permissions information is available at <http://www.nature.com/reprints>

Publisher's note Springer Nature remains neutral with regard to jurisdictional claims in published maps and institutional affiliations.

Open Access This article is licensed under a Creative Commons Attribution 4.0 International License, which permits use, sharing, adaptation, distribution and reproduction in any medium or format, as long as you give appropriate credit to the original author(s) and the source, provide a link to the Creative Commons licence, and indicate if changes were made. The images or other third party material in this article are included in the article's Creative Commons licence, unless indicated otherwise in a credit line to the material. If material is not included in the article's Creative Commons licence and your intended use is not permitted by statutory regulation or exceeds the permitted use, you will need to obtain permission directly from the copyright holder. To view a copy of this licence, visit <http://creativecommons.org/licenses/by/4.0/>.

This is a U.S. Government work and not under copyright protection in the US; foreign copyright protection may apply 2024